The band structure of the oxygen-octahedral ferroelectrics $BaTiO_3$, $SrTiO_3$, and $KTaO_3$, determined from data of two-photon spectroscopy

S. I. Shablaev, A. M. Danishevskiĭ, and V. K. Subashiev

A. F. Ioffe Physicotechnical Institute, Academy of Sciences of the USSR, Leningrad
(Submitted 2 September 1983)
Zh. Éksp. Teor. Fiz. **86**, 2158–2169 (June 1984)

In this paper we present two-photon absorption spectra of $BaTiO_3$, $SrTiO_3$, and $KTaO_3$ single crystals at various temperatures and for various polarizations of the light beam. These spectra show a strong similarity, which is a consequence of the interband nature of the two-photon optical transitions and the similarity between the band structures of these materials. An analysis of the temperature dependence of the spectra for various polarization configurations is carried out ($BaTiO_3$). The energy gaps and their temperature dependences for a number of direct and indirect transition edges are determined for the first time. A substantial splitting (~ 100 meV) is observed in various portions of the spectra, both for edge and deep states, at the phase transition in $BaTiO_3$ (for light polarization parallel to the axis of spontaneous polarization of the crystal). On the basis of the data obtained, a diagram of band-edge states and optical transitions is set up for these compounds on the actual energy scale. A comparison of the features of the two-photon spectra with various interband transitions within the framework of existing band structure calculations is carried out.

I. Crystals of $BaTiO_3$, $SrTiO_3$, and $KTaO_3$ belong to a group of oxygen-octahedral ferroelectrics having the perovskite structure (ABO_3). In the high-temperature phase all of them have O_h^1 cubic symmetry. In the ferroelectric phase transition ($T = 393$ K) in $BaTiO_3$ the unit cell is somewhat elongated along one of the fourfold axes, and its symmetry is reduced to C_{4v}^1. The phase transition also has a substantial effect on the band structure of $BaTiO_3$. It can lead to a shift and splitting of certain energy states.

In $SrTiO_3$ at 105–110 K there is a structural phase transition which lowers the symmetry of the crystal to D_{4h}^{18}, and in $KTaO_3$, without an external influence there are no phase transitions down to liquid helium temperatures.

Various calculations[1–4] have shown that the band structures of all the compounds of this group are very similar, with the lower states of the conduction band being built up on the basis of the $3d$ (for Ti) or $5d$ (for Ta) atomic orbitals of the transition metal, and the upper states of the valence band being formed from the $2p$ and, partially, of the $2s$ oxygen orbitals. In recent experimental investigations, using x-ray spectral and x-ray photoemission methods,[5] it was concluded that there is a strong hybridization of the titanium $3d$, $4s$, and $4p$ orbitals with the oxygen $2p$ orbitals, and that these states make a contribution to the valence band states. However, there are as yet no band structure calculations that take into account all these interactions.

Experimental investigations of the band structures of this group of compounds by optical methods have been carried out in a large number of works. A fairly complete review of these investigations is given in Refs. 2–4. Edge absorption and electroabsorption spectra have been studied, and in a wider spectral range, spectra of reflectance, electroreflectance, and thermoreflectance have been measured. Even though in almost all of these experimental investigations the authors compare their results with existing band-structure calculations,[1–4] the conclusions which they draw on the basis of the comparison, as well as the threshold energies for the optical transitions, differ widely among the various authors. The experimental transition threshold energies have been comparatively reliably established only for the relatively deep states. The band structure and the nature of the optical transitions directly after the fundamental absorption edge for this group of compounds have also been insufficiently studied.

Study of the band structure of the oxygen-octahedral ferroelectrics by the method of two-photon spectroscopy was begun in Ref. 6, in which an analysis of the two-photon absorption spectrum of $SrTiO_3$ at 295 K was carried out.[1)] In Ref. 7, two-photon absorption spectra of $BaTiO_3$ were taken for several temperatures and light polarizations. At the transition temperature in $BaTiO_3$ a polarization linear dichroism appears in the two-photon absorption spectra; this dichroism is associated with splitting of the bands as a result of the lowered symmetry of the crystal.

It was shown in Refs. 6 and 7 that the use of two-photon spectroscopy for the study of this group of materials is very informative, since several states, between which transitions occur, fall in the energy range in which two-photon spectra can be obtained.

In this work we obtain two-photon spectra of potassium tantalate and strontium titanate for a number of temperatures, we describe the results of the changes of the two-photon spectra of $SrTiO_3$ due to directed internal deformation or an applied electric field, and we compare the spectra of $SrTiO_3$, $BaTiO_3$, and $KTaO_3$. On the basis of the analysis of the spectra and their temperature and polarization behavior, we propose a model for the structure of the energy bands over the investigated energy range. The proposed model is compared with the band structure calculations published in Refs. 1–4.

 0038-5646/84/061256-08$04.00

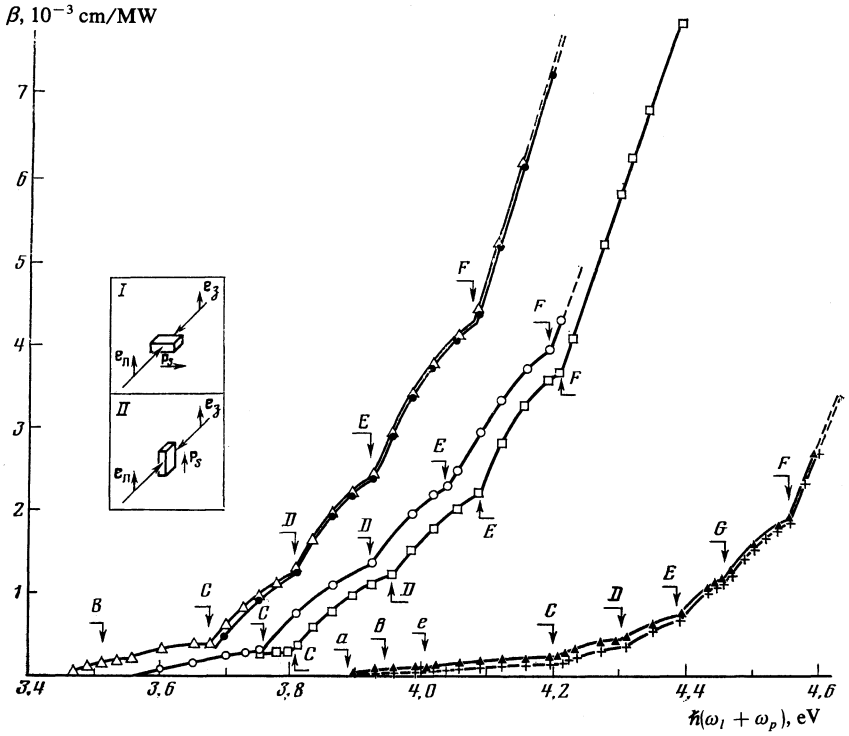

FIG. 1. Two-photon absorption spectra of $BaTiO_3$, $SrTiO_3$ and $KTaO_3$ crystals for various polarization configurations and temperatures.

$BaTiO_3$ { ● — 392 K, (I — $\mathbf{e}_l \| \mathbf{e}_p \perp \mathbf{P}_s$), ○ — 392 K, (II — $\mathbf{e}_l \| \mathbf{e}_p \| \mathbf{P}_s$), △ — 394 K, ($\mathbf{e}_l \| \mathbf{e}_p \| [001]$, } $SrTiO_3$ □ — 301 K; $KTaO_3$ { + — 298 K, ▲ — 399 K } $\mathbf{e}_l \| \mathbf{e}_p \| [001]$.

B is the edge for indirect transitions, *C*, *D*, *E*, *F*, and *G* are the edges for direct transitions, *A* and *E* are the threshold energies for transitions with the emission and absorption, respectively, of phonons. The insert shows the polarization configurations I and II for $BaTiO_3$.

II. Figure 1 shows the two-photon absorption spectra for the crystals $BaTiO_3$, $SrTiO_3$, and $KTaO_3$. For $BaTiO_3$, spectra are shown for the paraelectric phase at a temperature 394 K and for the ferroelectric phase at 392 K, for two polarization configurations.[2)] The spectra for $KTaO_3$ are shown for two temperatures, 298 and 399 K.

First of all, the similarity of structure of the two-photon absorption spectra of these crystals should be noted. This similarity is particularly noticeable for $SrTiO_3$ and $BaTiO_3$. Potassium tantalate is a wider-band crystal, and its two-photon absorption index β is considerably less than that of strontium or barium titanate for the same energy excess $\hbar\omega = h(\omega_l + \omega_p)$ above the threshold, (where ω_l and ω_p are the frequencies of the laser and probing radiation, respectively). This decrease in β for wider-band crystals is a specific property of two-photon absorption.

Each of the two-photon spectra in Fig. 1 consists of several segments with different slopes of β. In the vicinity of the edge of the spectra there are segments having very small slopes, and the values of β itself are also very small there.

The temperature behavior of these segments was analyzed and it was shown that these segments correspond to indirect two-photon transitions with the absorption and emission of a phonon. From this analysis the energies of the corresponding edges, the energy of the phonons, and the constant for the temperature variation of the energy gap were determined. In particular, it was found that in $BaTiO_3$ there is a single indirect edge, whereas in $SrTiO_3$ there are two (Fig. 2). In potassium titanate there is one indirect edge.

In each of the spectra there is a sharp break (indicated in the spectra by the letter *C*) in the higher energy region, and a considerable increase in the slopes of $\beta(\hbar\omega)$. A study of the temperature shift of this threshold and the attendant changes in the absolute values of β showed that the break in the spectrum corresponds to the direct transition edge in this group of materials.

The singularities (kinks) in the spectra at higher enegies we also associate with direct two-photon transitions[3)] into higher energy states. The basis for this conclusion is the parallel temperature shift of the spectra without significant change of β (in the paraelectric phase). The threshold energy for direct transitions for all the materials studied are shown in Table I. The threshold energies are indicated by the letters *C*, *D*, *E*, *F*, and *G*. It should be noted that there are four such

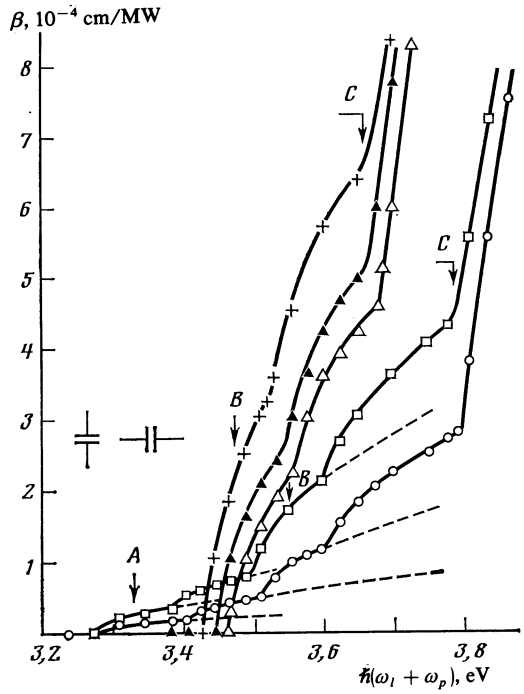

FIG. 2. Edge segments of two-photon absorption spectra of $BaTiO_3$ and $SrTiO_3$ for various temperatures.

$BaTiO_3$ { △ — 395 K, ▲ — 423 K, + — 468 K; $SrTiO_3$ { ○ — 301 K, □ — 423 K,

A and *B* are the edges for indirect transitions, *C* is the edge for direct transitions.

threshold energies for strontium and barium titanate in the range of energies investigated, and five for potassium tantalate.

The temperature behavior of the two-photon spectrum of $BaTiO_3$ (Fig. 1) is very typical of this material. At $T = 393$ K the crystal undergoes a phase transition. Across this transition, for polarization configuration I ($\mathbf{e}_l \| \mathbf{e}_p \perp \mathbf{P}_s$) there are practically no changes in the spectrum, while for configuration II ($\mathbf{e}_l \| \mathbf{e}_p \| \mathbf{P}_s$), all the spectra are considerably shifted to higher energies, with nonuniform shifts over different parts of the spectrum (in the above expressions, $\mathbf{e}_l$ and $\mathbf{e}_p$ are the polarization vectors of the laser and probe radiation, respectively, and $\mathbf{P}_s$ is the direction of spontaneous polarization). In Ref. 7 we have published spectra for $BaTiO_3$, taken over a wide temperature range. Those results make it possible to plot the temperature dependences of the above-mentioned threshold energies for both polarization configurations (Fig. 3). The symbol *B* in Fig. 3 denotes the indirect edge, for which the complete spectrum in the ferroelectric phase could be obtained only for polarization configuration II (because of interference due to the generation of the second harmonic in the crystal, it was not possible to distinguish the first part of the spectrum in configuration I).

III. In the analysis of the temperature behavior of the energy thresholds in the two-photon absorption spectra of barium titanate, it is noteworthy that the energy jump at the phase transition for polarization configuration II is the same for thresholds *D*, *E*, and *F*, while another energy jump is common to both *B* and *C*. Further, for all three high-energy thresholds in configuration II a practically uniform temperature shift towards short wavelengths is observed upon lowering the temperature in the ferroelectric phase. For energy thresholds *B* and *C* the analogous shift is considerably less. In addition, the ordinary temperature gradient of the energy gaps, observed in the paraelectric phase and in the ferroelectric phase for polarization configuration I and which are characterized by the value of $\partial E_i / \partial T$, are found to be identical for transitions *D*, *E*, and *F*. Transitions *B* and *C* also have identical gradients as a function of temperature, which, however, are somewhat larger in comparison with transitions *D*, *E*, and *F* (see Table I and Fig. 3).

This kind of temperature behavior for the energy thresholds can be explained by the fact that transitions *D*, *E*, and *F* occur in one part of the Brillouin zone and transitions *B* and *C* occur in another.

The energy shift of the spectrum towards higher energies at the phase transition for polarization configuration II and the absence of a shift in the case of configuration I is associated naturally with splitting of the bands (and the appearance of a spontaneous polarization) as a result of deformation of the unit cell. Here, transitions, corresponding to large band gaps, into the split-off states turn out to be forbidden for polarization configuration I and allowed for configuration II. The reverse holds for transitions between states which have not undergone an energy shift at the ferroelectric transition.

Taking into account that the temperature behavior is identical for transitions *D*, *E*, and *F*, we can propose that these transitions take place from three valence subbands to a single conduction band which also undergoes an energy splitting which increases with decreasing temperature in the ferroelectric phase. The identical temperature behavior of transitions *B* and *C*, one of which is indirect and the other direct, can also be explained on the basis of a model of transitions from different valence bands (the extrema of which are located in different points of the Brillouin zone) to a single conduction band whose temperature splitting in the ferroelectric phase also leads essentially to an energy splitting of

TABLE I. Edge energies and their temperature coefficients for direct transitions.

Crystal	C, eV	$\frac{\partial E_C}{\partial T}$, $\frac{\text{eV}}{\text{K}}$	D, eV	$\frac{\partial E_D}{\partial T}$, $\frac{\text{eV}}{\text{K}}$	E, eV	$\frac{\partial E_E}{\partial T}$, $\frac{\text{eV}}{\text{K}}$	G, eV	$\frac{\partial E_G}{\partial T}$, $\frac{\text{eV}}{\text{K}}$	F, eV	$\frac{\partial E_F}{\partial T}$, $\frac{\text{eV}}{\text{K}}$	T, K
$SrTiO_3$	3,79	$0{,}8\cdot10^{-4}$	3,96	$0{,}4\cdot10^{-4}$	4,08	$0{,}4\cdot10^{-4}$	–	–	4,21	$0{,}4\cdot10^{-4}$	423
$BaTiO_3$	3,67	$4\cdot10^{-4}$	3,80	$1{,}2\cdot10^{-4}$	3,92	$1{,}0\cdot10^{-4}$	–	–	4,08	$1{,}0\cdot10^{-4}$	423
$KTaO_3$	4,20	$1{,}3\cdot10^{-4}$	4,30	$1{,}0\cdot10^{-4}$	4,38	$1{,}0\cdot10^{-4}$	4,46	$1{,}0\cdot10^{-4}$	4,55	$1{,}0\cdot10^{-4}$	399

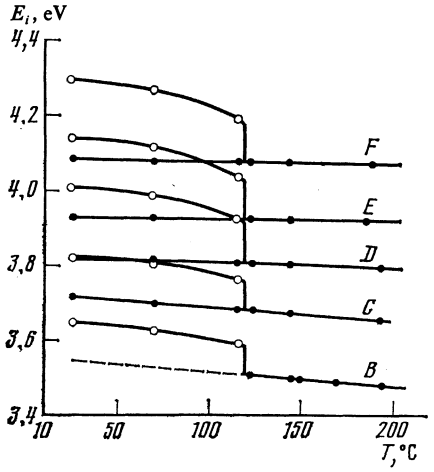

FIG. 3. Temperature dependences of the energies of the transitions *B*, *C*, *D*, *E*, and *F* of $BaTiO_3$ crystal for polarization configurations I (●) and II (○), (see caption to Fig. 1).

the spectra for the two polarization configurations.

IV. Existing band structure calculations[4] predict that the minimum interband energy gap for direct transitions in the perovskites ($BaTiO_3$, $SrTiO_3$, and $KTaO_3$) are located at the Γ and X points of the Brillouin zone (Fig. 4). It can be seen from the band diagram shown here that the lowest conduction band is the approximately flat band from $\Gamma_{25'}$ to X_3, while for the highest valence band the energy values for the points Γ, X, R, and M are about the same. In addition, at the top of the valence band there are a number of close-lying subbands at these points. However, the energy differences among these subbands (and the relative ordering of the points X, R, and M) are quite different in different calculations. The accuracy of the calculation does not permit a reliable determination of either the character of the edge absorption or of the position of the minimal extremum of the conduction band (the Γ or X point). Therefore, to construct the structure of the edge bands on the basis of the two-photon spectroscopy data, we shall use only those conclusions from the band structure calculations that practically coincide in all these investigations.

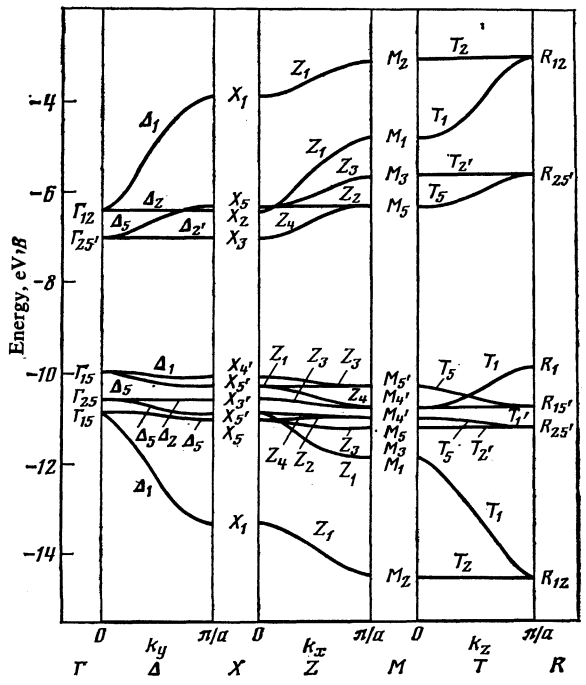

FIG. 4. Band structure of $SrTiO_3$ from Ref. 1.

We assume, in particular, that the transitions *B*, *C*, *D*, *E*, and *F* that are observed in $BaTiO_3$ occur at the Γ or X points of the Brillouin zone. Considering that in the majority of band structure calculations the valence band maximum located at the Γ point is considerably higher than at the X point, and assuming that the conduction band is practically flat along the direction from Γ to X, we reason that the first direct transition (and the associated indirect transition *B*) occur at the Γ point of the Brillouin zone. The flat character of the band is corroborated by the fact that in these materials the indirect transitions that we have observed are associated only with one extremum in the conduction band and not with two, as would be the case if the conduction band energies at the Γ and X points were appreciably different.

In accordance with the above discussion, we locate the lattermost direct optical transitions *D*, *E*, and *F* at the point X.

Thus, the analysis of the experimental data obtained allows us to draw some conclusions concerning the band structure of the perovskites studied. Namely:

1) The absorption edge in these materials is indirect, with a single indirect edge in $BaTiO_3$ and $KTaO_3$ and two in $SrTiO_3$.

2) The direct transitions *C*, *D*, *E*, and *F* occur at different points of the Brillouin zone, specifically Γ (transition *C*) and X (transitions *D*, *E*, and *F*).

3) Transitions *D*, *E*, and *F* are from three valence subbands to a single conduction band.

4) For linearly polarized light, the optical transitions *D*, *E*, and *F* take place at the centers of the Brillouin zone boundaries which are perpendicular to the direction of polarization of the light (for more detail, see section VII).

On the basis of these conclusions we have constructed a diagram of the band states at high symmetry points of the Brillouin zone (Fig. 5a) for $BaTiO_3$ on the true energy scale. The arrows indicate all the transitions we have observed between initial and final states corresponding to the energy thresholds of the two-photon spectrum. The energy levels drawn in with solid lines are for $BaTiO_3$. The left hand side of Fig. 5a shows the band diagram for this crystal in the paraelectric phase (O_h^1) (at 395 K) and on the left hand side is shown the diagram for $BaTiO_3$ in the ferroelectric phase (C_{4v}^1) at 392 K.

We based our conclusions on the fact that in the ferroelectric phase the extremum of the conduction band at the Γ point is split, while the extremum of the conduction band at the center of the Brillouin zone boundary which is perpendicular to the axis of tetrahedral distortion (at the Z point) is shifted towards higher energy, whereas at the zone boundaries that are parallel to this axis (at the X point) there is no shift.

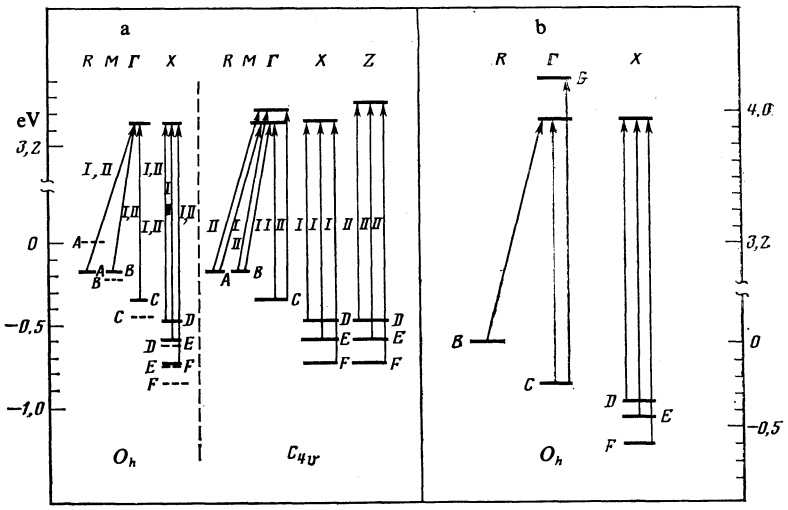

FIG. 5. Energy band diagram of crystals $BaTiO_3$, $SrTiO_3$, and $KTaO_3$. *A*, *B*, *C*, *D*, *E*, *F*, and *G* are band states associated with the corresponding two-photon transitions. Γ, *X*, *R*, *M*, and *Z* are high-symmetry points in the Brillouin zone. a) solid lines: absorption levels of $BaTiO_3$ in the paraelectric phase (O_h^1) and the ferroelectric phase (C_{4v}^1) for configurations I and II, $T = 392$ K. dashed lines: $SrTiO_3$, (O_h), $\mathbf{e}_l \| \mathbf{e}_p \| [001]$, $T = 395$ K; b) solid lines: $KTaO_3$, (O_h) $\mathbf{e}_l \| \mathbf{e}_p \| [001]$, $T = 399$ K.

In constructing the energy band diagram we have assumed that the indirect two-photon transitions corresponding to thresholds *A* and *B* for $SrTiO_3$ and *B* for $BaTiO_3$ originate from the top of the valence band at the points *R* and *M* of the Brillouin zone. This assumption stems from the fact that the band structure calculations[1-3] predict that the extrema of the valence band at these points are close in energy, and according to Ref. 4, the highest-lying points of the valence band are there (at *R* and *M*). We have previously noted that for $BaTiO_3$ there is only one indirect transition (*B*) at the edge, while for $SrTiO_3$ there are two (*A* and *B*). The difference in the strengths of the indirect transition *B* for $BaTiO_3$ and $SrTiO_3$ (see Fig. 2) are noteworthy. These strengths are determined by the value of β for $BaTiO_3$ and by the contribution to β from transition *B* in $SrTiO_3$ for the same energy excess of the quanta over the threshold energy. This difference is easy to account for if we assume that the valence band extrema at the *R* and *M* points in $BaTiO_3$ coincide in energy, so that the indirect transition *B* occurs at both these points in the conduction band, and as a consequence the transition also has a large strength, while on the other hand in $SrTiO_3$ these points differ in energy, so that in this material there are also two indirect transitions.

V. The diagram which we have constructed for the band states and the optical transitions on the basis of the investigation of the temperature and polarization dependence of the two-photon absorption spectra of $BaTiO_3$ should also apply in essence to $SrTiO_3$ and $KTaO_3$ (by virtue of the generality of the calculated band structures and the similarity of the two-photon spectra). To verify this we have carried out additional experiments involving various influences on the $SrTiO_3$ crystal.

In the first case, measurements were made of two-photon absorption spectra for a crystal which was cut along the cubic axes and to which an electric field was applied along the [100] direction. The spectra were taken for the two above-mentioned polarization configurations I and II. With this external electric field acting on the crystal one can expect an effect similar to that which occurs at the phase transition in $BaTiO_3$, i.e., an elongation of the unit cell of the crystal and the appearance of a spontaneous polarization due to the relative shift of the Ti and O sublattices. We did observe a small shift (5–10 meV) of the two-photon spectrum towards the high-energy region for polarization configuration II and no shift for configuration I, i.e., the picture is qualitatively similar to that of the behavior of the two-photon absorption spectrum of $BaTiO_3$ in the ferroelectric phase.

In the second case, a similarly cut $SrTiO_3$ crystal was subjected to an overall compression deformation which, however, was less along one of the [001] axes than along the other two.[5)] The result of this compression was the formation of an optical axis due to the quasi-tension in this direction. The two-photon spectra obtained for these crystals for configurations I and II (polarization configurations defined with respect to the optical axis), showed a substantial splitting (~ 30 meV) of the spectrum towards higher energies for configuration II relative to the spectrum for configuration I, i.e., in this experiment also the shift of the spectrum for the two polarization configurations was similar to that observed for $BaTiO_3$.

On the basis of these investigations we can conclude that the band diagram we have worked out is applicable to the explanation of the edge optical transitions in $SrTiO_3$ (indicated by the dashed lines in the diagram of Fig. 5a), and, possibly, in other perovskites.

VI. In the investigation of the edge absorption in $KTaO_3$ it was observed that in the two-photon spectra, in the region of direct absorption, there are five direct transitions, and not four as in the case of $BaTiO_3$ and $SrTiO_3$. We have indicated this "extra," fifth, transition by the letter *G*. To determine where this transition is located, it is necessary to refer back to the complete two-photon absorption spectra of the materials studied (see Fig. 1) and notice that after threshold *F* the dependence of β on the energy of the quanta is linear, whereas after thresholds *C*, *D*, and *E* it is a square root

dependence for all the perovskites investigated. Thus, these thresholds (F) correspond to transitions between analogous band states in all three perovskites. On the basis of this observation we have assumed that the extra transition in $KTaO_3$ is associated with one of the thresholds that lie between C and F. The appearance of the extra transition is logically associated with the replacement of Ti in the first two perovskites by Ta in $KTaO_3$ (here we have assumed that the band edges are formed from orbitals of the transition metal and of oxygen[1]). This replacement can lead to, among other things, a substantial spin-orbit splitting of the conduction band at the Γ point, since for Ta the spin-orbit splitting is large.[6)] Therefore, optical transitions associated with the spin-orbit splitting-off of the subbands should occur at the G point and, consequently, should be separated from threshold C by an amount equal to the spin-orbit splitting in this crystal. The best candidate is the threshold separated from C by 270 meV and which we have designated G.

In accordance with the discussion and reasoning which we have presented, we have constructed an energy band diagram for potassium tantalate in a true energy scale (Fig. 5b). This diagram indicates all the transitions B, C, D, E, F, and G which we have observed (for a temperature 399 K).

It should be emphasized that the presence of just five thresholds in the two-photon absorption spectrum of $KTaO_3$ confirms the correctness of the energy band diagram which we have proposed. An alternate version of the diagram, in which the transition from three valence subbands to the conduction band would be located at the Γ point in the diagram, would, in the case of potassium tantalate, lead to six energy thresholds because of the spin-orbit splitting of the conduction band. With the expected energy of this splitting, only four of these thresholds would fall in the measured range of the $KTaO_3$ spectrum, with the transition F coinciding in energy with the transition from the top of the valence subband to the spin-orbit split-off subband of the conduction band. Thus, the extra threshold in the $KTaO_3$ spectrum would appear.

VII. In order to identify the band diagram we have constructed from the experimental data (Fig. 5), with the specific symmetries of the states that enter into the theoretical calculations, it is necessary to analyze the possible two-photon transitions within the framework of the calculated band models.

The two-photon interband transitions in these crystals when they are in the paraelectric phase (O_h^1 symmetry) can be mainly of the permitted-forbidden type since almost all the states in the valence band and the conduction band have opposite parity.[1-4]

The selection rules for a two-photon transition are determined by the selection rules of the single-photon transitions that comprise it. The selection rules for allowed—forbidden transitions are essentially determined by the corresponding rules for the one-photon permitted transition, which we have also analyzed.

When the symmetry is lowered to C_{4v}^1 as a result of the phase transition in $BaTiO_3$ or external action on $SrTiO_3$, the degenerate valence band and conduction band states at Γ become split. Thus, the Γ_{15} state is split into Δ_1 and Δ_5 and the Γ_{25}, state into Δ_2 and Δ_5.

In the tetragonal phase of $BaTiO_3$ optical transitions for light polarized parallel to the axis of tetragonal distortion, the z axis, are allowed between the states Δ_5^v and Δ_5^c, and for polarization perpendicular to this axis, transitions are permitted between Δ_1^v and Δ_5^c as well as between Δ_5^v and $\Delta_{2'}^c$ (Fig. 6). Therefore, in order to explain the splitting we have observed in the two-photon absorption spectra for polarization configurations I and II, where the splitting occurred without a change in the shape of the spectra relative to the spectrum in the paraelectric phase, it is necessary to assume that the splitting in the conduction band ($\Delta_{2'}^c - \Delta_5^c$) and the valence band ($\Delta_1^v - \Delta_5^v$) are the same, since if they were not, one would expect additional thresholds in the two-photon absorption spectrum for configuration I, and these are not observed experimentally.

This character of the optically forbidden transitions in the ferroelectric phase of $BaTiO_3$ supports the correctness of the band transition diagram that we have chosen, since if the transitions D, E, and F were located at the Γ point, then in order to explain the experimentally observed splitting it would be necessary to assume identical splittings of one state in the conduction band and three states in the valence band. Such an assumption is unreasonable, since the states in the valence band have different symmetry, and there is no basis for assuming that they have the same splitting.

The selection rules for one-photon interband transitions at the X point of the Brillouin zone (only the $X_{4'}^v - X_3^c$ transition is forbidden) allows us to obtain various combinations of two-photon allowed—forbidden transitions where the interband transition from any of the valence subbands (see Fig. 4) to one of the branches of the conduction band will be allowed one.

With tetragonal distortion of the crystal in the direction of the z axis, the degenerate states will be split and the nondegenerate states will undergo energy shifts. In this case the band states at the X (1, 0, 0) and X(0, 1, 0) points of the ferroelectric phase and at the Z (0, 0, 1) point, which are formed as a result of the tetragonal distortion (the middle of the Brillouin zone boundary in the direction of the tetragoinal distortion), are shifted and split unequally. We assume that the minimum of the conduction band at the Z (0, 0,

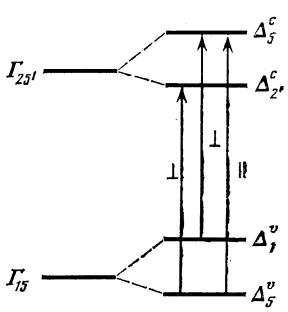

FIG. 6. Diagram of splitting of edge band states Γ_{15} and Γ_{25}, into Δ_5^v, Δ_1^v, $\Delta_{2'}^c$, and Δ_5^c resulting from tetragonal distortion of the crystal structure. The arrows show the optical transitions permitted for light polarized parallel (∥) and perpendicular (⊥) to the tetragonal axis.

1) point is shifted towards higher energy (reckoned from the top of the valence band) relative to the minima at the X (1, 0, 0) and X (0, 1, 0) points, which do not change in energy in the tetragonal distortion of the crystal structure, and we also assume that the valence band states are practically unshifted. This same result was obtained in a theoretical calculation[8] (for transitions on the Z_4–Z_2 line) of the effect on the band structure due to a displacment $\Delta\rho$ of the oxygen atoms relative to the center of the O–Ti–O chain along the polarization axis z.

The authors of Ref. 8 took into account only the change in the overlap integrals ($pd\pi$) and ($pd\sigma$) of the wave functions and they ignored the effect on the matrix elements due to a change in the bond angles between the atoms. Under these assumptions the tetragonal distortion affects only the levels at the boundaries perpendicular to the direction of the displacement, while all the levels at the boundaries parallel to the displacement do not change their energy. In this case the optical transitions are split into two series which are permitted for light polarized, respectively, parallel and perpendicular to the tetragonal axis z.

Our two-photon spectroscopy experiments for $BaTiO_3$ support such a model of band changes (at the X point of the Brillouin zone) in the perovskites in the ferroelectric phase, since the observed polarization splitting of the spectra of β are explained most simply on the basis of this model. Here it is necessary that the two-photon transitions D, E, and F be permitted between states at the Brillouin zone boundaries perpendicular to the direction of light polarization, and forbidden between states on zone boundaries parallel to the polarization direction. These transitions could be the allowed–forbidden transitions $X_{5'}^{v}$–X_2^c and $X_{5'}^{v}$–X_5^c, for which this condition is satisfied (while for transitions to X_3^c it is not satisfied). However, we have previously noted that the transitions D, E, and F most likely should be associated with a single conduction band whose shift in energy is determined by the polarization splitting in the spectra of β. Moreover, the representations of X_5^v and $X_{5'}^c$ are two-dimensional, and for tetragonal distortion can be not only shifted in energy (at the Z point) but also split [at the X (1, 0, 0) and X (0, 1, 0) points]. Therefore it is necessary to assume that these splittings of $X_{5'}^{v}$ and $X_{5'}^c$ are either small or the same (then an additional threshold will not appear in the spectrum of β for polarization configuration I).

Thus, the representations appearing in the calculations at the X point do not permit a satisfactory explanation of the polarization variations of the two-photon absorption spectra in the ferroelectric phase ($BaTiO_3$). In particular it is not possible to find in the valence band three states (for transitions D, E, and F) connected with a single conduction band state. This situation may be due to the simplified nature of the band structure calculations of these compounds and, in particular, to the neglect of the hybridization of the titanium $3d$, $4s$ and $4p$ orbitals with the oxygen $2p$ orbitals and the contribution of them to the valence band states.

Furthermore, the considerable difference we have observed in the band gap ($\sim$0.1 eV) and the character of the edge absorption for $BaTiO_3$ and $SrTiO_3$ (see Figs. 1 and 2, and Table I) are most probably a consequence of the effect of the Ba and Sr orbitals in the formation of the band edge states. In the theoretical calculations this effect was also neglected.

VIII. Let us consider also the question of the band gap. We have previously noted that in these crystals allowed-forbidden transitions occur. For interband absorption, without taking into account the Coulomb interaction, the spectral dependence of the two-photon absorption in the case of parabolic bands is described by the expression[9] $\beta \sim (\hbar\omega - E_i)^{3/2}$. Allowance for the Coulomb interaction in the two-band model[10] leads to an approximately linear dependence. However, in the spectra we have presented, all the segments except the last one have an approximately square-root dependence. Here the widths of these segments are relatively small: 0.1–0.15 eV for $SrTiO_3$ and $BaTiO_3$. This can be explained only by the fact that the bands have a strong nonparabolicity associated with their narrowness. Furthermore, from the temperature dependences of the spectra of $KTaO_3$ (Fig. 1 of this article) and of $BaTiO_3$ (Ref. 7), it can be seen that the temperature-induced rise of the spectra in the region of the indirect transition does not lead to a rise in the threshold points in the high-energy region. Thus, the value of β at the threshold point D in $BaTiO_3$ practically does not increase with increasing temperature. This means that at the energy at which the transition D takes place, the contribution to the absorption from transition B is already insignificant. On this basis we can also estimate the widths of these bands: $\sim 0.2 \pm 0.1$ eV. Their narrowness and quasi-two-dimensional character are confirmed by theoretical calculations.[11]

IX. Thus, in this paper we have presented two-photon spectra of $KTaO_3$, $BaTiO_3$ and $SrTiO_3$ and given an analysis of their temperature behavior for different polarization configurations ($BaTiO_3$). We have determined for the first time the energy gap for a number of indirect and direct transitions in these crystals, and have found the coefficients that determine their temperature-induced shifts. We have observed the energy splitting of the various segments of the spectra at the phase transition in $BaTiO_3$, both for the edge and for the deep states. On the basis of the data we have constructed a two-photon transition diagram. We have made a comparison of the features of the two-photon spectrum with various interband transitions in the framework of existing band structure calculations.

The authors thank I. P. Areshev and E. L. Ivchenko for discussions of a number of questions relating to the symmetry of the two-photon transitions.

[1)]Reference 6 describes also the experimental apparatus we made for the measurement of two-photon absorption spectra. The two-light-beam method was used; one of the beams was produced by a high-power pulsed aluminum-yttrium garnet laser and the other, the probe beam, by a pulsed lamp.

[2)]The experiments were carried out on a three-dimensional single-domain uncolored $BaTiO_3$ crystal.

[3)]For this investigation we chose samples with no contribution of two-step

one-photon processes. This was checked by the usual methods of two-photon spectroscopy.

[4)]Band-structure calculations of such complicated compounds are carried out using simplified models[1-3] where a number of parameters are used to produce a fit. An example is the ionicity of O and Ti (Ta); these are chosen so as to obtain a band gap E_g that agrees with the value known from experiment. However, the experimental values of E_g determined from an analysis of one-photon absorption spectra, which have an exponential character, cannot be determined with sufficient accuracy. Furthermore, the authors of the theoretical calculations did not take into account that the edge transitions in these materials are indirect.

[5)]Such a deformation is obtained by quenching (sudden nonequilibrium cooling of the crystal after annealing.

[6)]In the majority of the band structure calculations of the perovskites, spin-orbit splitting is not taken into account, but its value in the crystal is estimated by the spin-orbit splitting in Ti atoms for $BaTiO_3$ and $SrTiO_3$ and Ta atoms for $KTaO_3$. For Ti it is relatively small: ~20–30 meV, but for Ta it is relatively large: ~300 meV. The spin-orbit splitting in oxygen atoms is smal (~6–8 meV) and therefore it can be neglected in the valence band of the crystals studied.

[1]A. H. Kahn and A. I. Leyendecker, Phys. Rev, **135**, A1321 (1964).
[2]L. P. Mattheiss, Phys. Rev. **B6**, 4718 (1972).
[3]F. M. Midhel-Calendini and G. Mesnard, Phys. Status Solidi (b) **44**, K117 (1971); J. Phys. C **6**, 1709 (1973). P. Pertosa and F. M. Michel-Calendini, Phys. Rev. **B17**, 2011 (1978).
[4]T. Wolfram, E. A. Kraut, and F. J. Morin, Phys. Rev. **B7**, 1677 (1973).
[5]L. V. Shevchenko, E. A. Zhuravskiĭ, and K. S. Proskura, Ukr. Fiz. Zh. **27**, 1659 (1982).
[6]S. I. Shablaev, A. M. Danishevskiĭ, and V. K. Subashiev, Fiz. Tverd. Tela (Leningrad) **21**, 1140 (1979) [Sov. Phys. Solid State **21**, 662 (1979)].
[7]S. I. Shablaev, A. M. Danishevskiĭ, and V. K. Subashiev, Izv. Akad. Nauk SSSR ser. Fiz. **47**, 723 (1983) [Bull. Akad. Sci. USSR Phys. Ser. **47**, No. 4, 96 (1983)].
[8]J. D. Zook and T. N. Casselman, Phys. Rev. Lett. **17**, 960 (1966).
[9]R. Braunstein and N. Ockman, Phys. Rev. **134**, A499 (1964).
[10]G. D. Mahan, Phys. Rev. **170**, 825 (1968).
[11]T. Wolfram, Phys. Rev. Lett. **29**, 1383 (1972).

Translated by J. R. Anderson